Structural, electronic, and optical properties of $ZnO_{1-x}Se_x$ alloys using first-principles calculations*

Muhammad Rashid[a], Fayyaz Hussain[a]†, Muhammad Imran[a], S A Ahmad[a], N A Noor[b], M U Sohaib[d], and S M Alay-e-Abbas[c]

[a] Department of Physics Simulation Laboratory, the Islamia University of Bahawalpur, 63100, Pakistan
[b] Department of Physics, University of the Punjab, Quaid-e-Azam Campus, 54590 Lahore, Pakistan
[c] Department of Physics, GC University Faisalabad, Allama Iqbal Road, Faisalabad 38000, Pakistan
[d] Lahore Development Authority, 54590 Lahore, Pakistan

(Received 17 October 2012; revised manuscript received 25 December 2012)

The structural, electronic, and optical properties of binary ZnO, ZnSe compounds, and their ternary $ZnO_{1-x}Se_x$ alloys are computed using the accurate full potential linearized augmented plane wave plus local orbital (FP-LAPW + lo) method in the rocksalt (B1) and zincblende (B3) crystallographic phases. The electronic band structures, fundamental energy band gaps, and densities of states for $ZnO_{1-x}Se_x$ are evaluated in the range $0 \leq x \leq 1$ using Wu–Cohen (WC) generalized gradient approximation (GGA) for the exchange–correlation potential. Our calculated results of lattice parameters and bulk modulus reveal a nonlinear variation for pseudo-binary and their ternary alloys in both phases and show a considerable deviation from Vegard's law. It is observed that the predicted lattice parameter and bulk modulus are in good agreement with the available experimental and theoretical data. We establish that the composition dependence of band gap is semi-metallic in B1 phase, while a direct band gap is observed in B3 phase. The calculated density of states is described by taking into account the contribution of Zn 3d, O 2p, and Se 4s, and the optical properties are studied in terms of dielectric functions, refractive index, reflectivity, and energy loss function for the B3 phase and are compared with the available experimental data.

Keywords: density functional theory, alloys, structural, electronic, optical properties

PACS: 73.20.At, 78.20.Ci **DOI:** 10.1088/1674-1056/22/8/087301

1. Introduction

Group II–VI semiconductors have been a subject of intense research work due to their wide band gaps[1–4] that are important for their utilizations in optoelectronic and commercial electronic devices which operate in blue to near ultraviolet (UV) regions[5,6] The II–VI semiconductors are lucid for short wavelength optoelectronic applications in light emitting diodes (LEDs) and in laser diodes (LDs).[7] The outcome of the research work on these materials has resulted in improved LEDs and LDs working in the blue spectral region.[8] Compared with the earlier research interest in III–V semiconductors pertaining to their high luminescence efficiency and long life time, nowadays, the increased interest in II–VI semiconductors is due to their efficient use in various ultraviolet optoelectronic devices.[9]

ZnO is a highly promising material used for optoelectronic devices like LEDs, LDs transparent thin film transistors, and solar blind photo detectors.[10] It is also promising material for band gap engineering and spintronic applications.[11] In some earlier studies, the band gap engineering for ZnO has been reported in terms of selenium (Se) dopant.[12,13] Importantly, Salami *et al.*'s[14] and Guang *et al.*'s[15] theoretical studies regarding the ferromagnetism in nanosized and bulk ZnO have aroused the renewed research interest in doped ZnO. The direct band gap and transparency over a wide range of the visible spectrum are the properties which make ZnSe an attractive material.[16] The possible application of bulk ZnSe as femtosecond laser and $ZnSe/Zn_xCd_{1-x}Se$ heterostructures for electronic and optical properties makes pure and doped ZnSe promising materials for basic and applied research.[17,18]

The bowing parameters of ZnOSe alloys have been reported to be comparatively large and comparable with those of GaNAs and GaNP because of large electronegativity differences between O and Se atoms.[19,20] Quemard *et al.*'s theoretical study[21] for ZnO_xSe_{1-x} alloys shows that it is possible to have a ZnOSe ternary alloy with a larger band gap of equal chemical composition of Se in ZnO. On the other hand, the experimental analysis in terms of Raman spectrum of $ZnO_{1-x}Se_x$ is also available in Ref. [22]. To the best of our knowledge, no theoretical investigations of optical and electronic properties of $ZnO_{1-x}Se_x$ ternary alloy have been performed. In this paper, rocksalt (B1) and zincblende (B3) ZnO compound are doped with Se to calculate the structural and electronic properties of $ZnO_{1-x}Se_x$ ($x = 0$, 0.25, 0.50, 0.75, 1.0) in B1 and B3 phases, while the optical properties are studied for the first time in B3 phase. Accurate full potential linearized augmented plane wave plus local orbital (FP-LAPW + lo) method within the framework of density functional theory (DFT) is used as DFT calculations have time and again

*Project partially supported by HEC, Pakistan.
†Corresponding author. E-mail: fiazz_hussain@yahoo.com
© 2013 Chinese Physical Society and IOP Publishing Ltd

provide useful information about electronic and optical profile ternary compounds.[23,24]

2. Method of calculation

The FP-LAPW + lo method has been adopted for the calculations of structural, electronic, and optical properties of $ZnO_{1-x}Se_x$ using the WIEN2K code.[25] The total energy of the electrons is calculated by the exchange–correlation potential within the generalized gradient approximation (GGA) proposed by Wu and Cohen (WC).[26] The Kohn–Sham equation[27] is solved to determine the exchange–correlation energy for computing structural, electronic, and optical properties of $ZnO_{1-x}Se_x$ alloys. The potential and wave function are enlarged in spherical harmonic functions within the non-overlapping spheres containing the atomic sites (muffin tin spheres) R_{MT} (the radius of the muffin tin sphere) values used in this work are 2.2 a.u. for Zn, 2.06 a.u. for Se and 1.96 a.u. (a.u. is the abbreviation for atomic unit) for O which are selected in such a manner that there is no charge leakage from the core and total energy convergence is ensured. The charge density is Fourier expanded up to $G_{max} = 14$ (Ry)$^{1/2}$ and the maximum value for the wave function expansion inside the spheres is confined to $l_{max} = 10$. For the binary compounds ZnO and ZnSe the value of $K_{max} \times R_{MT} = 7$ is used while for the ternary $ZnO_{1-x}Se_x$ alloys $K_{max} \times R_{MT} = 8$ is used to find the energy eigenvalue convergence, where R_{MT} represents the smallest atomic sphere radius and K_{max} is the maximum value of the reciprocal lattice vector $\boldsymbol{k}$ in the plane wave expansion. The $\boldsymbol{k}$-mesh used in this work consists of 72 $\boldsymbol{k}$-points for binary and 35 $\boldsymbol{k}$-points for ternary alloys in both B1 and B3 phases. The dielectric function is analyzed by using a finer $\boldsymbol{k}$-mesh with 120 $\boldsymbol{k}$-points in the B3 phase. Self-consistency has been achieved when the difference in total energy between two consecutive cycles is less than 0.00001 Ry (1 Ry = 13.605 eV).

3. Results and discussion

3.1. Structural properties

In order to evaluate the structural properties of $ZnO_{1-x}Se_x$ alloys at $x = 0.0$, 0.25, 0.5, 0.75, and 1.0, we first calculate the structural properties of the end binary ZnO and ZnSe in the B1 and B3 phases that belong to space groups Fm-3m and F-43m, respectively. The space groups of $ZnO_{1-x}Se_x$ at $x = 0.25$ and 0.75 are Pm-3m in B1 and P-43m in B3, while for $x = 0.50$ the structure becomes tetragonal with space group $P4/mmm$ in B1 and P-4m2 in B3 phase. The volume optimization is done by minimizing the total energy at a number of different volumes. Using the Murnaghan's equation of state (EOSs)[28] we compute the equilibrium structural parameters such as the lattice parameter (a_0) and the bulk modulus (B) for binary and their alloys. The volume optimization curves of $ZnO_{1-x}Se_x$ alloys at $x = 0.25$, 0.50, and 0.75 are shown in Fig. 1. The computed results of structural parameters are summarized in Tables 1 and 2, where it can be seen that our present calculations of end binaries are in reasonable agreement with the experimental and other calculated values that are obtained using other GGA functionals. The lattice parameters of $ZnO_{1-x}Se_x$ alloys in both phases increase by increasing the concentration of Se and the bulk modulus decreases. The values of the lattice parameter and bulk modulus for $ZnO_{1-x}Se_x$ alloys of Se concentration are presented in Fig. 2, for both phases respectively. It is also noticed that with varying concentration lattice constant shows a considerable deviation from Vegard's law[29] which is comparatively large for the bulk modulus.

Table 1. Calculated lattice parameters and bulk modulus of $ZnO_{1-x}Se_x$ alloys compared with experimental and other theoretical results in B1 phase.

Composition	Lattice constant a/Å			Bulk modulus B/GPa		
x	this work	expt.	other calculations	this work	expt.	other calculations
0	4.342	4.271[a]	4.337[b], 4.334[c]	162.41	228[a]	161.45[b], 167.8[c]
0.25	4.661			121.86		
0.50	4.963			99.432		
0.75	5.117			91.947		
1	5.301	5.299[d]	5.268[e]	80.397	104.0[d]	78.6[e], 77.84[f]

[a]Ref. [30], [b]Ref. [31], [c]Ref. [32], [d]Ref. [33], [e]Ref. [34], [f]Ref. [35]

Table 2. Calculated lattice parameters and bulk moduli of $ZnO_{1-x}Se_x$ alloys compared with experimental and other theoretical results in B3 phase.

Composition	Lattice constant a/Å			Bulk modulus B/GPa		
x	this work	expt.	other calculations	this work	expt.	other calculations
0	4.623	4.62[g]	4.616[b], 4.633[c]	131.64	163.241[g]	125.34[b], 133.73[c]
0.25	4.987			92.233		
0.50	5.348			81.203		
0.75	5.449			73.064		
1	5.738	5.667[h]	5.623[i]	59.801	69.311[h]	68.9[i], 63.07[j]

[b]Ref. [31], [c]Ref. [32], [e]Ref. [34], [f]Ref. [35], [g]Ref. [36], [h]Ref. [37], [i]Ref. [38], [j]Ref. [39]

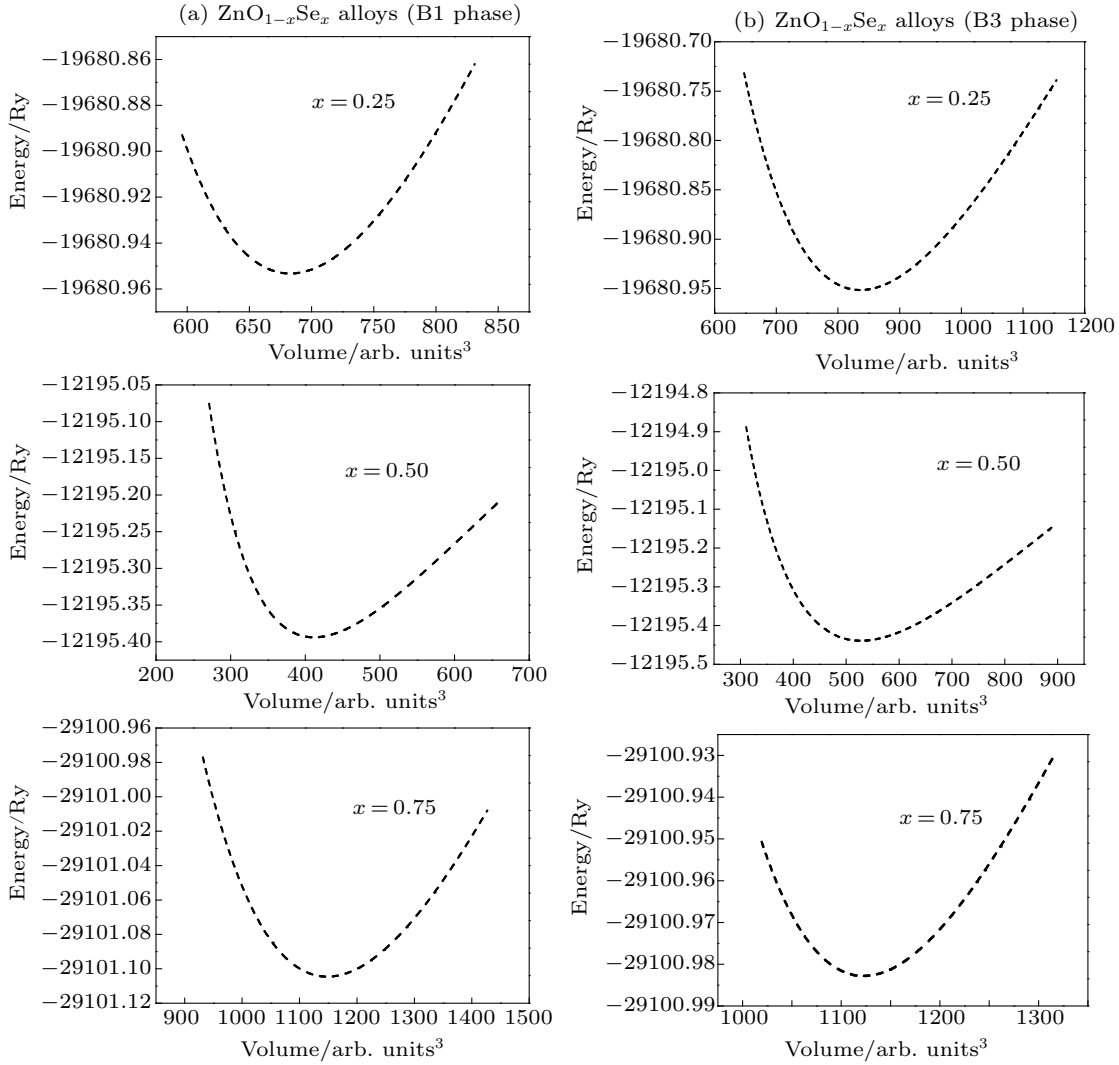


Fig. 1. Structural optimization plots for $ZnO_{1-x}Se_x$ alloys at $x = 0.25$, 0.50, and 0.75 in (a) B1 phase and (b) B3 phase.

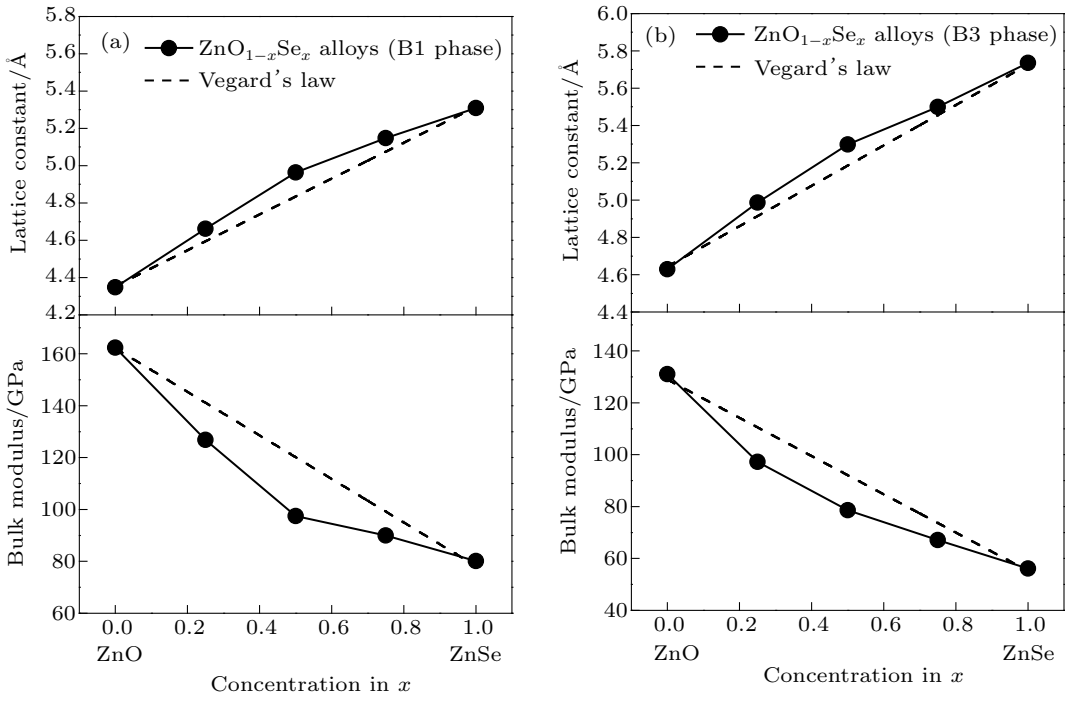


Fig. 2. Variations of the calculated lattice parameters and bulk moduli with x for $nO_{1-x}Se_x$alloys (a) in B1 and (b) B3 phase.

3.2. Electronic properties

In one way or another, the physical properties of a compound are based on the electronic band structure of a material, where the cause of the band structure lies in the density of state (DOS). So a rigorous understanding of band gaps and band structures necessarily becomes vital for the development of optoelectronic, magneto–optic and magneto–electronic devices. For the electronic band structure calculations, the Zn-3d, 4s, O-2s, 2p, and the Te-4s , 4p states are taken as valence states and all low lying states are treated as part of the core. In B1 phase, band structure calculations show a metallic behavior except at ZnO (i.e. $ZnO_{1-x}Se_x$ at $x = 0$) that has an indirect-band-gap (Γ–X). In the case of B3 phase, the band structure shows a direct band-gap (Γ–Γ) behavior for $ZnO_{1-x}Se_x$ at concentrations of $x = 0.0$, 0.25, 0.5, 0.75, and 1.0.

ZnO compound in B1 phase has valance band maximum along the L-direction that touches the Fermi surface while the conduction band minimum is along the X-direction 0.9 eV above the Fermi surface. Hence, there is a small indirect band gap in the ground state but in B3 phase our calculations show that it is a direct band-gap material (the conduction band minimum (CBM) and valence band maximum (VBM) are located at the Γ-symmetry point). On the other hand, the band structure of ZnSe in the B1 phase reveals that the valance band touches the Fermi surface and along the X-direction the conduction band goes below the Fermi surface. Hence, the material shows metallic nature while in ZB phase the direct-band-gap the conduction band minimum (CBM) and valence band maximum (VBM) located at the Γ-symmetry point) of semiconductor nature are observed. For the ternary alloy $ZnO_{1-x}Se_x$, the band structure in B1 phase indicates that both conduction and valence bands overlap and the material has a metallic nature (Fig. 3), while in B3 phase the band gap decreases continuously with the increase of Se concentration. It can be observed from Fig. 4 that the band gap energy value decreases with the increase of Se concentration which is consistent with the results in earlier work.[40] The band gap energy decreases from 1.26 eV to 0.76 eV with composition increasing from 0.25 to 0.75 for B3 phase. The calculated band-gap (Γ–Γ) values for B3 phase as a function of Se concentration is shown in Fig. 6, which are in good agreement with the experimental results.[41]

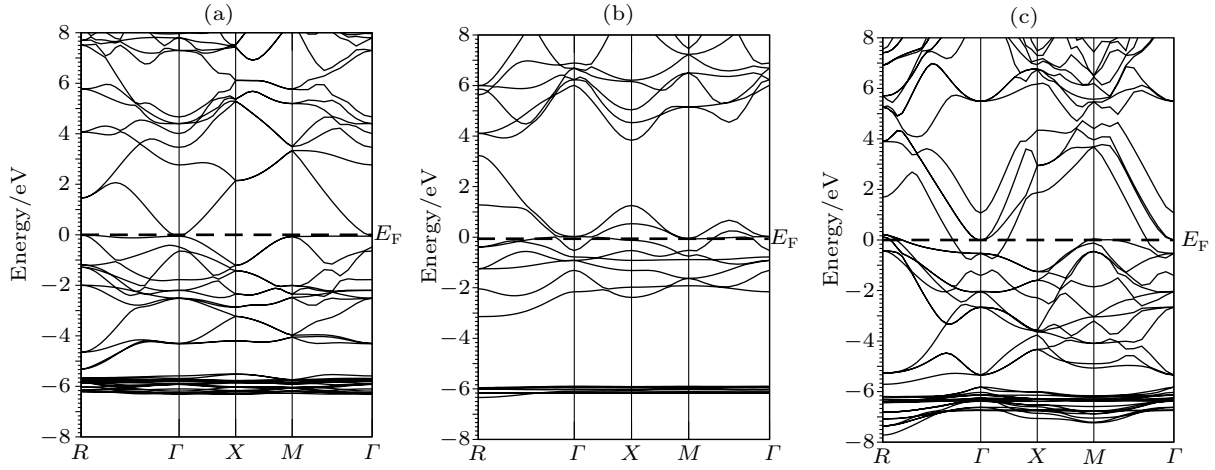


Fig. 3. Band structures of (a) $ZnO_{0.75}Se_{0.25}$, (b) $ZnO_{0.50}Se_{0.50}$, and (c) $ZnO_{0.25}Se_{0.75}$ in B1 phase.

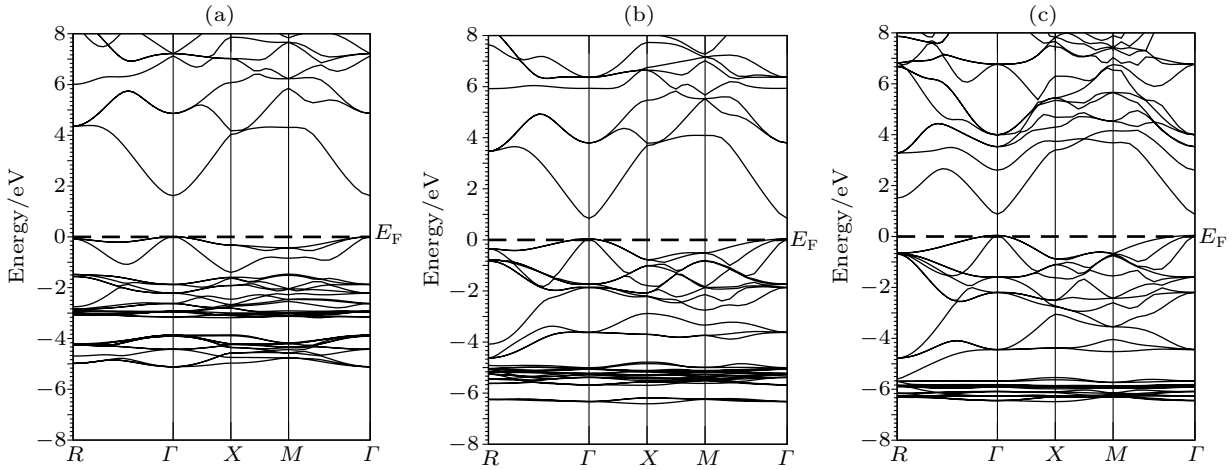


Fig. 4. Band structures of (a) $ZnO_{0.75}Se_{0.25}$, (b) $ZnO_{0.50}Se_{0.50}$, and (c) $ZnO_{0.25}Se_{0.75}$ in B3 phase.

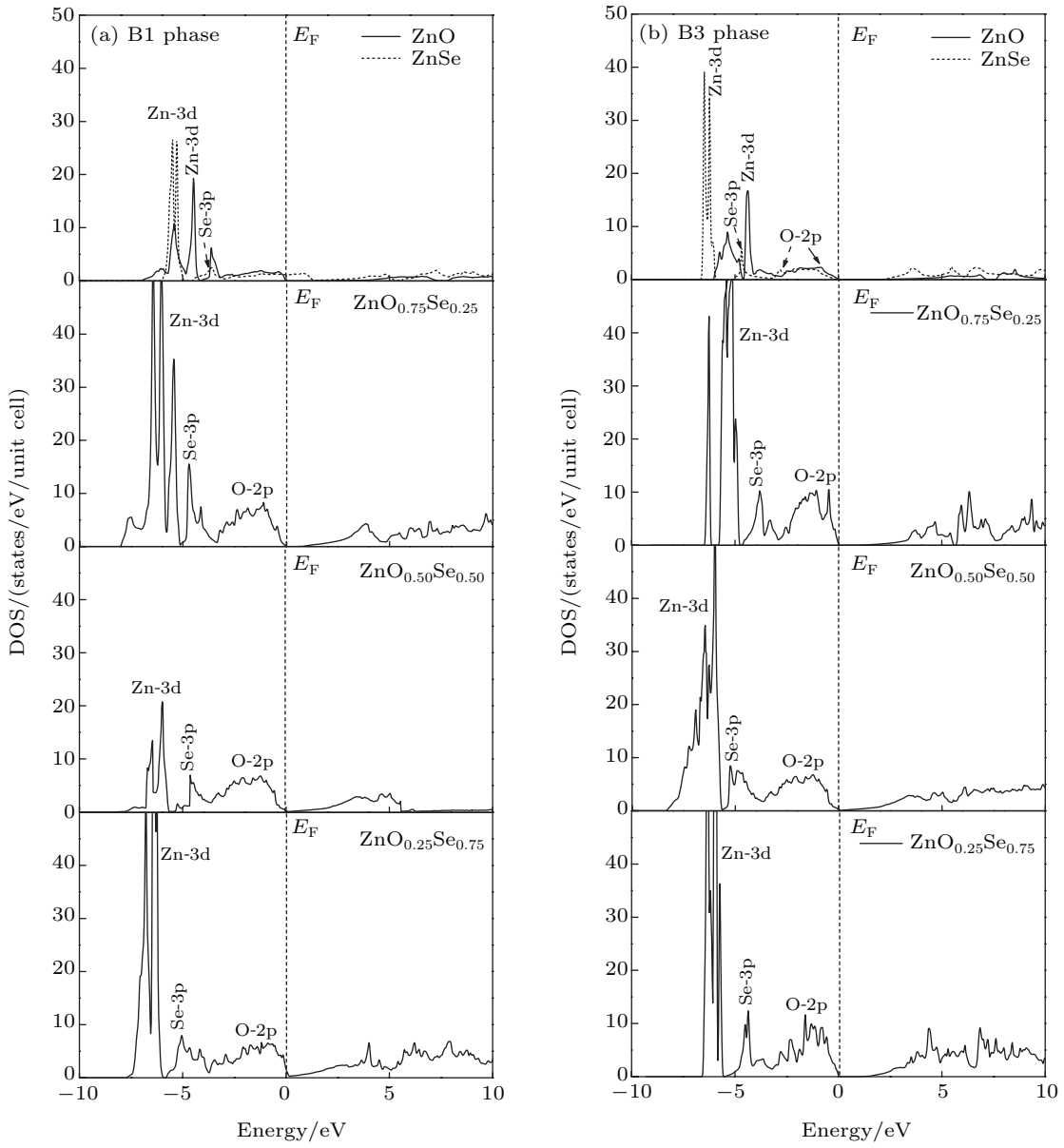


Fig. 5. Total densities of states (TDOSs) of $ZnO_{1-x}Se_x$ alloys at $x = 0.0$, 0.25, 0.50, 0.75, and 1, (a) in B1 phase and (b) B3 phase.

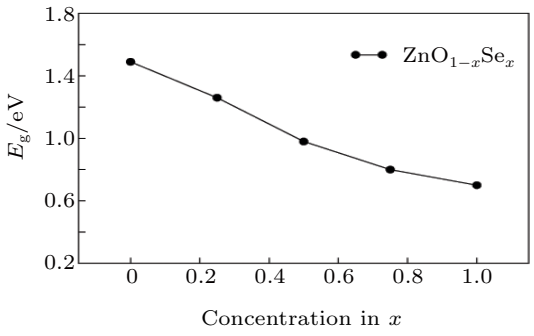


Fig. 6. Band gap values of $ZnO_{1-x}Se_x$ alloys in B3 phase at $x = 0.0$, 0.25, 0.50, 0.75, and 1.

The electronic DOSs for $ZnO_{1-x}Se_x$ alloys ($x = 0$, 0.25, 0.50, 0.75, 1.0) in B1 and B3 phases provide a further insight into the contributions of various states to the conduction and valence bands. The valence electronic configurations of Zn, O, and Se are $3d^{10}\ 4s^2$, $1s^2\ 2s^2\ 2p^4$, and $3d^{10}\ 4s^2\ 4p^4$ respectively. Total DOS along with the partial DOS of Zn, O, and Se for $ZnO_{1-x}Se_x$ in B1 and B3 phases are shown in Figs. 5(a) and 5(b). For both ZnO and ZnSe compounds, there are large contributions of Zn 3d, O 2p, Se 4s states in the valence band and Se 4p states in the conduction band, therefore both compounds in B1 phase do not show any distinct energy gap having metallic nature, while in B3 phase they exhibit semiconducting nature with distinctive energy gap. Figures 5(a) and 5(b) each demonstrate the extra peak that appears between −5 eV and 0 eV in valence band during alloy formation with compositions $x = 0.25$, 0.50, and 0.75 separately. For the alloy system, the lower part of valence band is totally dominated by the contribution of Zn 3d, Se 4s states, while upper part near the Fermi level is occupied by O 2p, state. We can see that the alloy system retains the metallic nature in B1 phase, whereas semiconducting nature in B3 phase. The DOSs in B1 and B3 phases show that the Zn-3d states are broadened between −3 eV and −6 eV and according to the photoemission dimen-

sions, the Zn-3d states should be situated at about −6 eV at valence band.[42]

3.3. Optical properties

Theoretically, the optical properties of $ZnO_{1-x}Se_x$ alloys have not been studied yet but some results are obtained experimentally.[22] As the calculation of optical properties in the spectral range plays a vital role in the profound understanding of the nature of that material, this information directly provides a transparent picture for the usage of this material in optoelectronic devices. By considering that the core properties of $ZnO_{1-x}Se_x$ alloys that are direct band gap semiconductors make them optically active material all respective properties like frequency-dependent dielectric functions, refractive index, reflectivity, and energy loss function are probed in detail to cover their practical usage in optoelectronics.

The optical properties of matter can be calculated by complex dielectric function $\varepsilon(\omega) = \varepsilon_1(\omega) + i\varepsilon_2(\omega)$, where $\varepsilon_1(\omega)$ and $\varepsilon_2(\omega)$ are the real and imaginary components of the dielectric function, respectively. The electronic band structure is directly related to the imaginary part $\varepsilon_2(\omega)$ and it can be calculated by adding all possible occupied states to the unoccupied states of transitions. A complete explanation of the calculation of these elements is given by Ambrosch–Draxl and Sofo.[43] The real part $\varepsilon_1(\omega)$ can be derived from the imaginary part using the Kramers–Kronig transformation. For B3 phase, the imaginary part calculations of the dielectric function for $ZnO_{1-x}Se_x$ for $x = 0.0$, 0.25, 0.50, 0.75, and 1.0 are shown in Fig. 8(a). It is observed that $\varepsilon_2(\omega)$ seems to be the same for all Se concentrations with some changes that are discussed in detail. It is observed that ZnO has durable absorption region from 3.2 eV to 14.0 eV, while ZnSe has strong absorption region from 4.3 eV to 8.5 eV. The initial critical points of $\varepsilon_2(\omega)$ occur at about 2.8, 1.4, 1.0, 0.9, and 0.76 for $ZnO_{1-x}Se_x$ alloys with $x = 0.0$, 0.25, 0.50, 0.75, and 1.0, respectively and are recognized to be the thresholds for the direct optical transitions occurring at 1.49, 1.26 , 0.98, 0.80, and 0.70 eV. We observe that the values of $\varepsilon_2(\omega)$ for all the binary and ternary alloys are naturally shifted towards lower energies with the amplitude increasing as Se concentration increases. This confirms our results that the increase in Se concentration causes a decrease in band gap. The real part calculations of the dielectric function are shown in Fig. 8(b).

An important quantity of $\varepsilon_1(\omega)$ is the zero frequency limit $\varepsilon_1(0)$. It represents the dielectric response to the static electric field. In $ZnO_{1-x}Se_x$, $\varepsilon_1(0)$ increases from 2.6 to 4.2 and the direct band gap decreases as x increases from 0 to 1. These features of $\varepsilon_1(0)$ are closely related to the real part of the complex refractive index $n(\omega)$. Penn model[44] is suitable for understanding the dependence of the dielectric function on energy gap. This model provides the relation $\varepsilon(0) \approx 1 + (\hbar\omega_p/E_g)^2$ where ω_p is the plasma frequency and E_g is the energy band gap; it clearly depicts the inverse proportion relation between dielectric function and band gap. A recent experiment on ZnOS:Al films has also shown a similar behavior of decreasing dielectric constant with the increase of optical energy gap.[22] With the increase in Se concentration, the first solid peak in $\varepsilon_1(\omega)$ shifts to a higher incident photon energy, then a sharp reduction is observed.

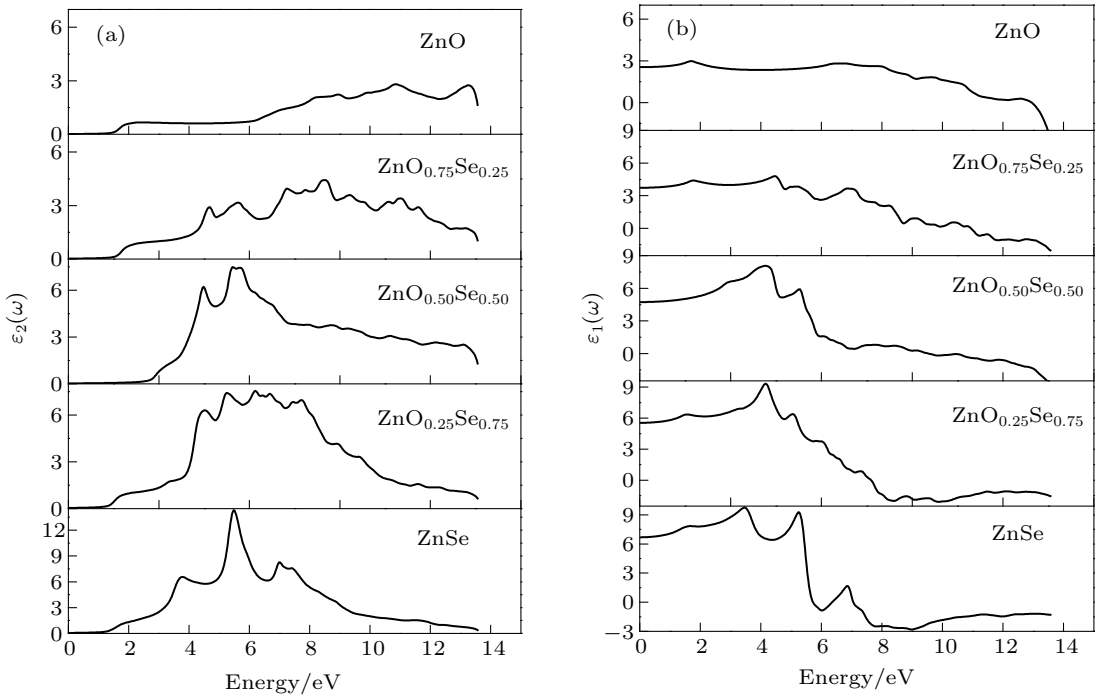


Fig. 7. Dielectric constants for $ZnO_{1-x}Se_x$ alloys corresponding to different values of x for (a) $\varepsilon_2(\omega)$ and (b) $\varepsilon_1(\omega)$.

Figure 8(a) shows the plots of refractive index $n(\omega)$ for $ZnO_{1-x}Se_x$ alloys at concentration $x = 0.0$, 0.25, 0.50, 0.75, 1.0 and the values of $n(0)$ for their corresponding zero frequency range are given in Table 3. As the concentration increases, zero frequency $n(0)$ also increases. Our results clearly show that there is an inverse relation between the direct band gap and $n(0)$. This explains lower $n(\omega)$ for the wide bandgap semiconductor. For ZnSe, our calculated values of $n(\omega)$ are reliable in comparison with the experimental results.[41,45] The reflectivity co-efficient $R(\omega)$ depends on $\varepsilon_1(\omega)$ and $\varepsilon_2(\omega)$. The maximum peak of $R(\omega)$ occurs after 13 eV for each concentration as shown in Fig. 8(b). It means that beyond 13 eV, maximum reflection appears. Finally, the electron energy-loss function $L(\omega)$ can also be obtained from $\varepsilon_1(\omega)$ and $\varepsilon_2(\omega)$. The spectra of energy loss do not show any distinctive maximum peak in the region of about 0 eV–2.5 eV. In the range about 11.5 eV–12.8 eV, the peaks of energy loss are larger but slightly different from the peaks for $x = 0.5$ because it has a tetragonal structure.

Table 3. Calculated optical parameters for $ZnO_{1-x}Se_x$ at different Se concentrations.

x	$E_g^{\gamma-\gamma}$/eV	ε_1	$R(0)$	$n(0)$	ε_2 (critical values)
0	1.49	2.60	0.08	1.60	2.80
0.25	1.26	2.80	0.10	1.80	1.40
0.50	0.98	3.20	0.13	2.10	1.00
0.75	0.80	3.70	0.17	2.30	0.90
1	0.72	4.20	0.20	2.60	0.76

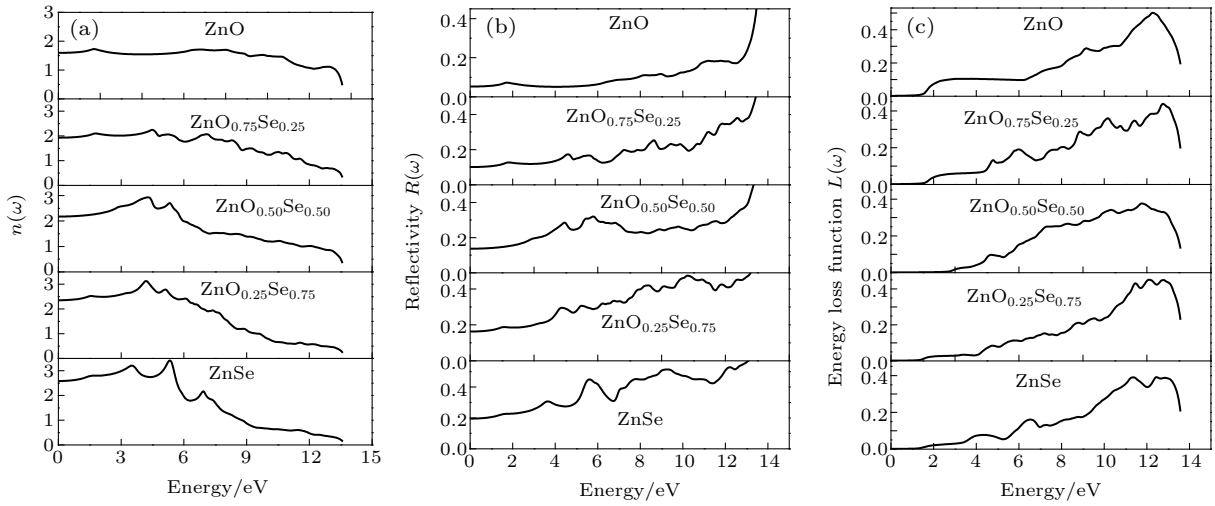


Fig. 8. Complex refractive indexes for $ZnO_{1-x}Se_x$ alloys corresponding to different values of x for (a) $n(\omega)$, (b) $R(\omega)$, and (c) $L(\omega)$.

4. Conclusions

In this study, we calculate the electronic band structures, DOSs, and optical properties for the $ZnO_{1-x}Se_x$ alloys using FP-LAPW + lo method within the framework of DFT. We find the direct band gap in B3 phase but metallic behavior in B1 phase for all Se concentrations. The DOS calculations for alloy system show that the Zn 3d and Se 4s states dominate the lower part of the valence band and O 2p state dominates the upper part of the valence band. Our calculated optical spectra of the alloy accord quite well with experimental data. The analysis of our results confirms the optical properties of the $ZnO_{1-x}Se_x$ alloys are improved with Se concentration increasing. Hence, our study may be regarded as a measurable theoretical prediction for such properties.

Acknowledgement

This work was done in Physics Department, Simulation Laboratory (SL), the Islamia University of Bahawalpur.

References

[1] Joseph M, Tabata H and H.Kawai H 1999 *J. Appl. Phys.* **1** 38
[2] Venkatesan M, Fitzgerald C B, Lunney J G and Coey J M D 2004 *Phys. Rev. Lett.* **93** 177
[3] Klingshirn C, Priller H, Decker M, Bruckner J, Kalt H, Hauschild R, Zeller J, Bakin A, Wehmann H, Thonke K, Sauer R, Kling R, Reuss F, and Kirchner C 2005 *Adv. Solid State Phys.* **45** 275
[4] Ozgur U, Alivov Y I, Liu C, Teke A, Reshchikov M A, Dogan S, Avrutin V, Cho S J and Morkoc H 2005 *J. Appl. Phys.* **98** 041301
[5] Freund H 2007 *J. Surf. Sci.* **601**1438
[6] Karami H, Aminifar A, Tavallali H and Namdar Z 2010 *Clust. Sci.* **21** 1
[7] Cho M W, Chang J H, Bagnall D M, Koh K W, Saeki S, Park S K T, Zhu Z, Hiraga K and Yao T 1999 *J. Appl. Phys.* **85** 512
[8] Van der Walle C G 1993 *Wide Band-gap Semiconductors* (Amsterdam: North Holland)
[9] Makino T, Segawa Y, Kawasaki M, Ohtomo A, Shiroki R, Tamura K, Yasuda T and Koinuma H 2001 *Appl. Phys. Lett.* **78** 1237
[10] Kang B S, Wang H T, Tien L C, Ren F, Gila B P, Norton D P, Abernathy C R, Lin J S and Pearton S 2006 *J. Sensors* **6** 643
[11] Long Z, Fei L P, Yuan Y Z, Jia M S, Lu D and Tao L J 2012 *Chin. Phys. B* **21** 097103
[12] Yoo Y Z, Jin Z W, Chikyow T, Fukumura T, Kawasak M and Koinuma H 2002 *Appl. Phys. Lett.* **81** 3798
[13] Shan W, Walukiewicz W, Ager J W III, Yu K M, Wu J, Haller E E, Nabetani Y, Mukawa T, Ito Y and Matsumoto T 2003 *Appl. Phys. Lett.* **83** 299

[14] Salmani E, Benyoussef A, Ez-Zahraouy H, Saidi E H and Mounkachi O 2012 *Chin. Phys. B* **21** 106601
[15] Guang X X, Ling Y H, Zhang Y Y, Lin D and Yong J 2012 *Chin. Phys. B* **21** 047504
[16] Hirose J, Uesugi K, Hoshiyama M, Numai T and Suemune I 1998 *J. Appl. Phys.* **84** 6100
[17] Li H Y, Jie W Q, Zhang S A, Sun Z R and Xu K W 2006 *Chin. Phys.* **15** 2407
[18] Ping B X and Liang B S 2008 *Chin. Phys. B* **17** 4606
[19] Iwata K, Fons P, Yamada A, Shibata H, Matsubara K, Nakahara K, Takasu H and Niki S 2002 *Phys. Stat. Sol. B* **229** 887
[20] Wei S H and Zunger A 1996 *Phys. Rev. Lett.* **76** 664
[21] Quemard G, Reiss P, Carayon S and Bleuse J 2005 *J. Crystal Growth* **275** 5
[22] Angelika P, Bruno K M, Thorsten K, Changzhong W and Axel H 2006 *Phys. Stat. Sol.* **203** 2868
[23] Noor N A, Ikram N, Ali S, Nazir S, Alay-e-abbas S M and Shaukat A 2010 *J. Alloys Compd.* **507** 356
[24] Dong Y X, Bing L, Feng L R, Lu W X and Xun Z 2011 *Chin. Phys. B* **20** 036104
[25] Blaha P, Schwarz K, Madsen G K H, Kvasnicka D and Luitz J 2001 *WIEN2K* (Vienna: Techn. Universitat)
[26] Wu Z and Cohen R E 2006 *Phys. Rev. B* **73** 235116
[27] Schwarz K, Blaha P and Madsen G K H 2002 *Comput. Phys. Commun.* **147** 71
[28] Murnagham F D 1944 *Proc. Natl. Acad. Sci.* **30** 244
[29] Vegard L 1921 *Z. Phys.* **5** 17
[30] Nazir S, Ikram N and Amin B 2009 *J. Phys. Chem. Solids* **70** 874
[31] Amin B, Ahmad I, Maqbool M, Ikram N, Saeed Y and Ahmad A 2010 *J. Alloys Compd.* **493** 212
[32] Karzel, Potzel H W, Kofferlein M, Schiessl W, Steiner M, Hiller U, Kalvius G M, Mitchell D W, Das T P, Blaha P, Schwarz K and Pasternak M P 1996 *Phys. Rev. B* **53** 11425
[33] Charifi, Baaziz Z H and Reshak A H 2007 *Phys. Stat. Sol.* **244** 3154
[34] Schleife A, Fuchs F, Furthmuller J and Bechstedt F 2008 *Phys. Rev.* **73** 245212
[35] Mujica A, Munoz A and Needs R J 1998 *Phys. Rev. B* **57** 1344
[36] Qteish A, Abu-Jafar M and Nazzal A 1998 *J. Phys.: Condens. Matter* **10** 5069
[37] Shouxin C, Haiquan H, Wenxia F, Chenb X and Feng Z 2009 *J. Alloys Compd.* **472** 294
[38] Bragg W H and Darbyshire J A 1954 *J. Met.* **6** 238
[39] Nelmes R J, McMahon M I, Wright N G and Allan D R 1995 *J. Phys. Chem. Sol.* **56** 545
[40] Labidi S, Meradji H, Labidi M, Ghemid S, Drablia S and Hassan F El Haj 2009 *Phys. Procedia* **2** 1205
[41] Nabetani Y, Mukawa T, Ito Y, Kato T and Matsumoto T 2003 *Appl. Phys. Lett.* **83** 299
[42] Mahdi S, Neda L and Roland H 2011 *J. Appl. Phys.* **109** 073705
[43] Ambrosch–Draxl C and Sofo J O 2006 *Comput. Phys. Commum.* **175** 1
[44] Penn D R 1962 *Phys. Rev.* **128** 2093
[45] Bhattacharyya S R, Gayen R N, Paul R and Pal A K 2009 *Thin Solid Films* **517** 5530